Macedonian Journal of Chemistry and Chemical Engineering, Vol. **38**, No. 2, pp. 253–266 (2019)

MJCCA9 – 784

ISSN 1857-5552
e-ISSN 1857-5625

Received: January 22, 2018
Accepted: November 21, 2019

DOI: 10.20450/mjcce.2019.1368
Original scientific paper

QUANTUM CHEMICAL STUDIES, SPECTROSCOPIC ANALYSIS AND MOLECULAR STRUCTURE INVESTIGATION OF 4-CHLORO-2-[(FURAN-2-YLMETHYL)AMINO]-5-SULFAMOYLBENZOIC ACID

C. Charanya[1], S. Sampathkrishnan[2], N. Balamurugan[3,*]

[1]*Research Scholar, Department of Physics, Sri Venkateshwara College of Engineering, Sriperumbudur 602105, Tamil Nadu, India*
[2]*Department of Physics, Sri Venkateshwara College of Engineering, Sriperumbudur 602105, Tamil Nadu, India*
[3*]*Department of Physics, Dhanalakshmi College of Engineering, Tambaram, Chennai, Tamil Nadu, India*
n_rishibalaa@yahoo.co.in

In this study, the FTIR, FT-Raman and UV-visible Spectra of furosemide molecule, $C_{12}H_{11}ClN_2O_5S$ (with named, 4-chloro-2-[(furan-2-ylmethyl)amino]-5-sulfamoylbenzoic acid), were recorded experimentally and theoretically. The optimized geometrical structure, harmonic vibration frequencies, and chemical shifts were computed using a hybrid-DFT (B3LYP) method and 6-31G(d,p) as the basis set. The complete assignments of fundamental vibrations were performed on the basis of the experimental results and Total Energy Distribution (TED) of the vibrational modes. The first order hyperpolarizability and relative properties of furosemide were calculated. The UV-Visible spectrum of the compound was recorded in the range 200–400 nm and the electronic properties, such as HOMO and LUMO energies, were determined by Time-Dependent DFT approach. Furthermore, Mulliken population analysis and thermodynamic properties were performed using B3LYP/6-31G(d,p) level for the furosemide compound.

Keywords: DFT; TED; UV-Vis; HOMO-LUMO

КВАНТНОХЕМИСКА СТУДИЈА, СПЕКТРОСКОПСКА АНАЛИЗА И ИСПИТУВАЊЕ НА МОЛЕКУЛСКАТА СТРУКТУРА НА 4-ХЛОРО-2-[(ФУРАН-2-ИЛМЕТИЛ)АМИНО]-5-СУЛФАМОИЛБЕНЗОЕВА КИСЕЛИНА

Во оваа студија беа експериментално снимени и теориски пресметани FTIR, FT-Raman и UV-vis спектрите на фуросемидната молекула $C_{12}H_{11}ClN_2O_5S$ (именувана 4-хлоро-2-[(фуран-2-илметил)амино]-5-сулфамоилбензоева киселина). Оптимизираната геометриска структура, хармониските вибрациони фреквенции и хемиските поместувања беа определени со хибриден метод на DFT (B3LYP) и базисен сет 6-31G(d,p). Целосната асигнација на фундаменталните вибрации беше извршена врз основа на експерименталните резултати и вкупната енергетска распределба (TED) на вибрационите модови. Беа пресметани хиперполаризабилноста од прв ред и релативните својства на фуросемидот. Беше снимен UV-Vis спектарот на соединението во опсегот од 200–400 nm и беа определени електронските својства како што се енергиите HOMO и LUMO по пат на временски зависен приод на DFT. Покрај тоа, беше извршена популациона анализа по Mulliken и беа определени термодинамички својства со примена на B3LYP/6-31G(d,p) ниво за фуросемидното соединение.

Клучни зборови: DFT; TED; UV-Vis; HOMO-LUMO

1. INTRODUCTION

Furosemide is a potent diuretic drug commonly used in adults, children and infants, for the management of excessive fluid accumulation and edema caused by congestive heart failure, renal disease, and cirrhosis of the liver. In adults, oral FURO may be used alone, or in combination with different antihypertensive agents, for the treatment of hypertension [1]. In addition, the unsubstituted aromatic/heterocyclic sulphonamides act as carbonic anhydrase inhibitors [2, 3] whereas other types of derivatives show diuretic activity (high-ceiling diuretics or thiadiazine diuretics), hypoglycemic activity, and anticancer properties [4]. Due to their significant pharmacology applications and widespread use in medicine, these compounds have gained attention in bio-inorganic and metal-based drug chemistry. Inter- and intramolecular hydrogen bonding interactions [5–7] have thus received an increased attention, both from a practical and a theoretical point of view, in determining the structure and activity of the biological molecule [8].

The Becke-3-Lee-Yang-Parr (B3LYP) functional provides an excellent agreement between the accuracy and computational efficiency of vibrational spectra of bioactive molecules [9–11]. A literature survey reveals that, to the best of our knowledge, the results based on quantum chemical calculations, vibrational spectral studies and HOMO-LUMO analysis on furosemide has not been reported. Hence, we wanted to make a spectroscopic characterization of the furosemide molecule with a view to get some insight into the structure function relationship through spectra-structure correlation. In order to achieve this objective, FT-Raman, FTIR and UV-visible spectroscopic studies, along with HOMO (the highest occupied molecular orbital) – LUMO (lowest unoccupied molecular orbital) analysis have been performed by applying density functional theory calculations based on Becke3-Lee-Yang-Parr (B3LYP) with 6-31G(d,p) as a basis set. Quantum chemical computational methods have proved to be an essential tool for interpreting and predicting the vibrational spectra [12, 13].

2. EXPERIMENTAL DETAILS

The furosemide compound, acquired from Lancaster Chemical Company, UK. was utilized accordingly for the spectral measurements. The FT-IR range of furosemide was recorded in a Bruker IFS 66 V spectrometer in the scope of 4000–400 cm^{-1}. The range was recorded at room temperature with a filtering velocity of 30 cm^{-1} min^{-1} and the spectral resolution of ± 2 cm^{-1}. The FT-Raman range of furosemide was additionally recorded in the scope of 4000–100 cm^{-1} utilizing a similar instrument with a FRA 106 Raman module furnished with a Nd:YAG laser source, working at 1.064 μm line widths with 200 mW control. The frequencies of every single sharp band are precise to ± 1 cm^{-1}. The ultraviolet absorption range of furosemide solved in water was analyzed in the range 200–400 nm by utilizing a Cary 5E UV – visible NIR recording spectrometer. All the spectral measurements were completed at the Indian Institute of Technology, Chennai, India.

3. COMPUTATIONAL DETAILS

In the present work, the Density Functional Theory (DFT/B3LYP) at the 6-31G(d,p) basis set level was adopted to calculate the properties of the furosemide molecule. All the calculations were performed using the Gaussian 09W program package [14] with the default convergence criteria without any constraint on the geometry [15]. The equilibrium geometry corresponding to the true minimum on the Potential Energy Surfaces (PES) has been obtained by effectively solving self-consistent field equations. The vibrational spectra of the furosemide were obtained by taking the second derivative of energy, computed analytically by the use of Total Energy Distribution (TED) using the SQM program [16, 17], along with the available related molecule.

4. RESULTS AND DISCUSSION

4.1. *Geometric structure*

The first task for the computational work was to determine the optimized geometry of the studied molecule. The optimized molecular structure of furosemide with the numbering scheme of the atoms was obtained from the Gauss View program [18]. The optimized geometrical parameters of furosemide calculated by DFT-B3LYP level with the 6-31G(d,p) basis set are listed in Table 1, which are in accordance with the atom numbering scheme given in Figure 1.

From the theoretical values one can find that most of the optimized bond lengths are larger than the experimental values. This overestimation can be explained in that the theoretical calculations belong to the isolated molecule in the gaseous phase and the experimental results belong to the molecules in the solid state.

T a b l e 1

The calculated geometrical parameters of 4-chloro-2-[(furan-2-ylmethyl)amino]-5-sulfamoylbenzoic acid bond lengths in angstrom(Å) and angles in degrees (°)

Bond lengths	Calculated values	Bond angles (°)	Calculated values
C1-C2	1.486	C2-C1-O8	120.058
C1-O8	1.227	C2-C1-O9	124.526
C1-O9	1.349	C1-C2-C3	122.376
C2-C3	1.414	C1-C2-C7	118.417
C2-C7	1.408	O8-C1-O9	115.416
C3-C4	1.408	C3-C2-C7	119.207
C3-C14	1.400	C2-C3-C4	118.272
C4-C5	1.395	C2-C3-C14	120.836
C4-H22	1.101	C2-C7-C6	122.353
C5-C6	1.405	C2-C7-H23	119.029
C5-Cl21	1.729	C4-C3-C14	120.892
C6-C7	1.398	C3-C4-C5	121.734
C6-S10	1.810	C3-C4-H22	119.698
C7-H23	1.102	C3-C14-C15	125.536
O9-H24	0.971	C3-C14-H27	116.717
S10-O11	1.453	C5-C4-H22	118.568
S10-O12	1.452	C4-C5-C6	120.382
S10-N13	1.689	C4-C5-H21	117.561
N13-H25	1.019	C6-C5-H21	122.055
N13-H26	1.019	C5-C6-C7	118.027
N14-C15	1.474	C5-C6-S10	123.456
N14-H27	1.046	C7-C6-S10	118.499
C15-C17	1.504	C6-C7-H23	119.029
C15-H28	1.114	C6-S10-O11	107.683
C15-H29	1.114	C6-S10-O12	108.277
O16-C17	1.368	C6-S10-N13	109.223
O16-C20	1.362	O11-S10-O12	116.021
C17-C18	1.367	O11-S10-O13	107.774
C18-C19	1.431	O12-S10-O13	108.981
C18-H30	1.095	S10-O13-H25	110.919
C19-C20	1.360	H25-O13-H26	111.479
C19-H31	1.096	C15-N14-H27	117.744
C20-H32	1.094	N14-C15-C17	111.096
O9-H27	1.882	N14-C15-H28	110.108
		N14-C15-H29	109.690
		C17-C15-H28	108.032
		C17-C15-H29	108.051
		C15-O16-C17	121.902
		C15-C17-C18	128.335
		H28-C15-H29	109.820

The changes in the bond length of the C-H bond of the substituents may be of the electron withdrawing type (Cl, F, Br, etc.) due to a change in the charge distribution on the carbon atom of the benzene ring, as has been explained by many authors [19–22]. The carbon and hydrogen atoms are bonded with a σ-bond in the benzene ring, and the substitution of a halogen reduces the electron density of the C atom. Therefore, substitution with Cl, Br or F at the C(5) atom, which shares its *p* electron with the ring, leads to some changes of the bond lengths and bond angles in the aromatic ring. It is well known that DFT methods predict bond lengths which are systematically too long, particularly the C-H and N-H bond lengths [23]. The theoretical bond lengths of C-H are in the range from

1.095 to 1.102 Å. Likewise, the calculated bond lengths of N-H are in the range from 1.01 to 1.11Å. The calculated bond lengths of C=C fall in the range from 1.395 to 1.405 Å. For the benzene-sulfonamide molecule, these bond lengths were found in the range 1.339 to 1.407 Å [24]. The computational method, B3LYP, which includes electron correlation effects, strongly overestimates all the bond lengths around sulfur [25–27]. In this study, the S-O bond lengths are predicated well by the DFT method.

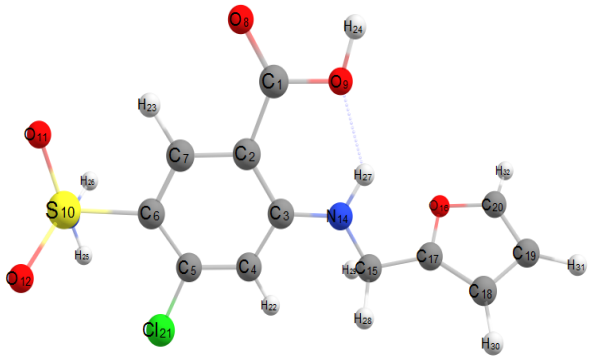

Fig. 1. The optimized geometric structure at the DFT/B3LYP/6-31G(d,p) level of 4-chloro-2-[(furan-2-ylmethyl)amino]-5-sulfamoylbenzoic acid

Substitution with halogen atoms and SO_2 leads to some changes of the bond angles in the aromatic ring. The C(5)-C(6)-C(7) angle at the position of the SO_2 substituent, and the C(4)-C(5)-C(6) angle at the position of the halogen substituent, are larger (118.01° and 120.30°, respectively), and the others are smaller than the typical hexagonal angle of 120°.

4.2. *Vibrational assignments*

The optimized structural parameters were used to compute the vibrational frequencies of furosemide at the DFT, B3LYP/6-31G(d,p) level of calculations. The molecule consists of 32 atoms which undergo 90 fundamental modes of vibrations associated with this furosemide molecule. All the 90 vibrations are in agreement with C_1 symmetry. Vibrational spectral assignments have been carried out on the recorded FTIR and FT-Raman spectra based on the theoretically predicted wavenumbers by B3LYP with the 6-31G(d,p) basis set, and the results, along with their TED values, are presented in Table 2. The experimental and theoretical FTIR and FT-Raman spectra were shown in Figures 2 and 3. The calculated wavenumbers are all positive values and confirm that the optimized structure of the furosemide molecule is the most stable conformer.

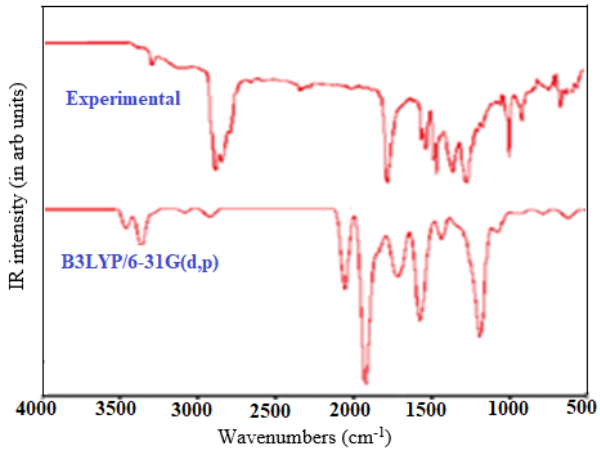

Fig. 2. Experimental and theoretical FTIR spectra of -chloro-2-[(furan-2-ylmethyl)amino]-5-sulfamoylbenzoic acid

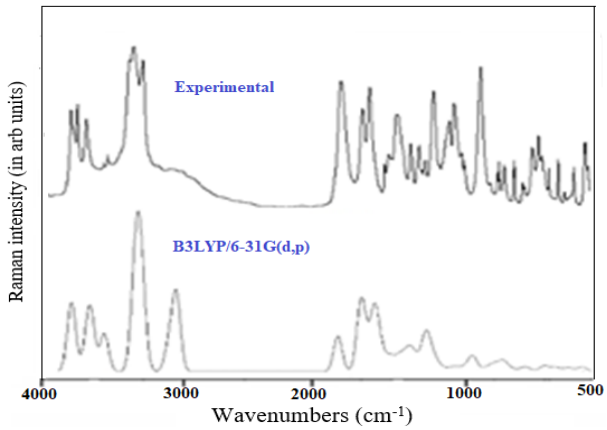

Fig. 3. Experimental and theoretical FT-Raman spectra of chloro-2-[(furan-2-ylmethyl)amino]-5-sulfamoylbenzoic acid

Some bands in the calculated FTIR spectra were not observed in the experimental spectrum. It is imported to note that computed wavenumbers correspond to the gaseous phase of an isolated molecular state, whereas the observed wavenumbers correspond to the solid state spectra. In order to determine the correlations between the calculated and experimental wavenumbers, the linear correlation coefficients (R^2) values, which were 0.9976 and 0.9962 for the FTIR and FT-Raman wavenumbers of the furosemide molecules, respectively, and the correlation graphics, are given in Figure 4.

T a b l e 2

Experimental and calculated wavenumbers (cm^{-1}) and their assignments of 4-chloro-2-[(furan-2-ylmethyl)amino]-5-sulfamoylbenzoic acid at the B3LYP/6-31G(d,p) level

Modes	Experimental		DFT/6-31G Calculated wavenumber		Vibrational assignment (TED > 10 %)
	FTIR	FT-Raman	Unscaled	Scaled	
1			3759.84	3616.97	υ OH (100)
2			3648.99	3510.33	υ OH (99)
3			3621.75	3484.12	υasym NH2 (100)
4	3380		3520.78	3386.99	υsym NH2 (98)
5			3299.17	3173.80	υsym CH (100)
6		3147	3274.31	3149.88	υsym CH (98)
7			3263.45	3139.44	υsym CH (95)
8			3245.92	3122.57	υsym CH (94)
9		3107	3233.73	3110.85	υasym CH_2 (92)
10		2930	3051.30	2935.35	υasym CH_2 (98)
11		2880	2996.29	2882.43	υasym CH_2 (97)
12	1650	1607	1817.63	1748.56	υ CC (89)
13			1659.00	1595.95	υ CC (80) + β CH (15)
14		1583	1646.56	1583.99	υ CC (72) + β CH (12)
15	1556		1615.48	1554.09	υ CC (80)
16	1531	1530	1588.35	1527.99	ρNH2 (89)
17			1568.35	1508.75	ρNH2 (80)
18			1533.14	1474.88	βCH_2 (67) + ν CC (26)
19	1456	1454	1514.16	1456.62	βCH_2 (61) + ν CC (23)
20	1423		1494.20	1437.42	ν CC (40) + β CH (37)
21			1460.61	1405.11	ν CC (39) + β CH (32)
22	1373	1370	1431.53	1377.13	ν CC (36) + β CH (34)
23			1399.38	1346.21	υsym SO_2 (86)
24	1316	1310	1364.00	1312.16	υasym SO_2 (48) + υ CC (30)
25			1360.06	1308.38	υasym SO_2 (53) + υ CC (37)
26			1322.05	1271.81	β CH (71) + υ CC (22)
27		1251	1303.96	1254.41	υasym SO_2 (40) + υ CC (40) + β CH (10)
28			1293.67	1244.51	B CH (43) + υasym SO_2 (40)
29			1281.91	1233.19	υCCl (48) + υ CC (21) + βCH (40)
30			1255.21	1207.51	B CH (71) + υ CC (19)
31			1233.99	1187.10	β CH (80) + υ CC (20)
32	1150	1160	1185.84	1140.78	β CH (38) + υ CC (34)
33			1181.02	1136.14	υ CC (33) + υasym SO_2 (40) + β CH (17)
34			1154.40	1110.53	υsym SO_2 (51)
35			1129.85	1086.92	β CH (71) + υ CC (19)
36			1119.89	1077.33	τ NH_2 (85) + υasym SO_2 (11)
37			1112.34	1070.07	τ NH_2 (75) + υasym SO_2 (10)
38			1094.15	1052.57	υ CC (28) + υasym SO_2 (24) + β CH (22)
39			1090.71	1049.26	υ CC (47) + β CCC (20) + β CH (20)
40	1005		1044.52	1004.83	γ CH_2 (97)
41	955		996.04	958.19	γ CH_2 (88)
42			984.25	946.85	γ CH_2 (82)
43			963.84	927.21	γ CH_2 (80)
44	906		944.58	908.69	γ CH_2 (82)
45			900.81	866.58	γ CH (70) + τ HCCCl (25)

T a b l e 2 – continue

46			882.03	848.52	γ CH(60) + τ HCCCl(15)
47			843.59	811.54	υ S-NH_2 (67)
48			836.62	804.83	γ CH(69) + τ CCCl(19) + τ CCS(12)
49			827.91	796.44	γ CH(68) + τ CCCl(19) + τ CCS(10)
50			818.19	787.10	υ CC(20) + υ CCl (18) + υ NS(15) + β CCC(10)
51			777.11	747.58	τ CCCC(30) + υ CCl(11) + υ CS(10)
52			754.52	725.85	τ CCCC(35) + τ CCC(11) + υ CCl(10)
53			741.49	713.31	τ CCCC(25) + τ CCC(11) + υ CCl(10)
54			697.83	671.31	τ CCC(54) + τ CCCH(15) + υ CCSO(12)
55			691.91	665.62	υCCC(48) + τCCH(10) + τ CCSO(12)
56			673.56	647.97	υ CS(32) + β CCC(18) + υ NS(11) + υ CCCl(10)
57			658.96	633.92	υ CS(25) + β CCC(15) + υ NS(11) + υ CCCl(10)
58			640.01	615.69	βCCC(56) + βCCH(17)
59			621.75	598.13	τHNO(30) + υ SN(29) + β HNSC(15) + τCSNH(12)
60			615.03	591.66	τHNO(28) + υ SN(25) + β HNSC(10) + τCSNH(11)
61			613.58	590.27	τHNO(20) + υ SN(15) + β HNSC(10) + τCSNH(11)
62			579.20	557.19	τHN(42) + υ CCCl(14) +υ CS(16)
63			547.65	526.84	τCSNH(35) + βCSO(15) + υ CCCl(10)
64			536.14	515.76	τCCCH(28) + τ CCSO(23) + τ CCCC(13) + υSN(10)
65			490.99	472.33	υCCl(40) + υCS(25) + τ HNSO(10)
66			474.64	456.61	υCCl(35) + υCS(10) + βCCC(10)
67			456.44	439.09	βNSO(32) + τCSNH(32) +βCSO(17) + τCCSN(10)
68			447.86	430.84	ρSO_2(34) + γSCC(25) + τNH_2(20)
69			434.43	417.93	γCCC(28) + τ NH_2(17)
70			400.35	385.14	βCCl(34) +βNH_2(10)
71			375.19	360.93	τ NH_2(43) + υ C-SO_2(12) + βCSO(11)
72			335.01	322.28	βCSN(30) + τCCCl(13) + τCCCS(12) + τHCCCl(10)
73			320.33	308.16	τ NH_2(46) + τ SO_2(22)
74			311.77	299.93	βCCCl(68) + τHSO(36) + βCSO(27)
75			298.19	286.85	βCCCl(57) + τHSO(26) + βCSO(17)
76			251.75	242.18	υCS(38) + βCCC(14) + υCCl(10)
77			242.88	233.65	υCS(28) + βCCC(10) + υCCl(10)
78			221.36	212.95	υCCl(25) + υCS(24) + βCCC(13)
79			205.12	197.33	βCSN(45) + τCCCl(34) + τCCCC(12) + τHCCCl(10)
80			189.60	182.40	βCSN(30) + τCCCl(24) + τHCCl(11) + τCCSO(10)
81			147.90	142.28	τHNSO(50) + βCCS(15) + βCCCl(12)
82			133.42	128.35	τNH_2(93)
83			120.52	115.94	τNH_2(90)
84			101.43	97.57	τCCCS(37) + τHCCS(15) + τCCl(10)
85			62.77	60.39	τCCCS(33) + τCCCCl(17) + τHCCSC(13)
86			55.24	53.15	τ ring SO_2(96)
87			51.49	49.53	τ ring SO_2(98)
88			50.21	48.30	τ ring SO_2(99)
89			27.15	26.12	τ CCSO(56) + τCCSN(40)
90			17.76	17.09	τ CCSO(58) + τCCSN(39)

Abbreviations used: vs – very strong, s – strong, m – medium, w – weak, vw – very weak; υ – stretching, α – deformation, B – in plane bending, γ – out of plane bending, ρ – rocking, ω – wagging and τ – twisting/torsion

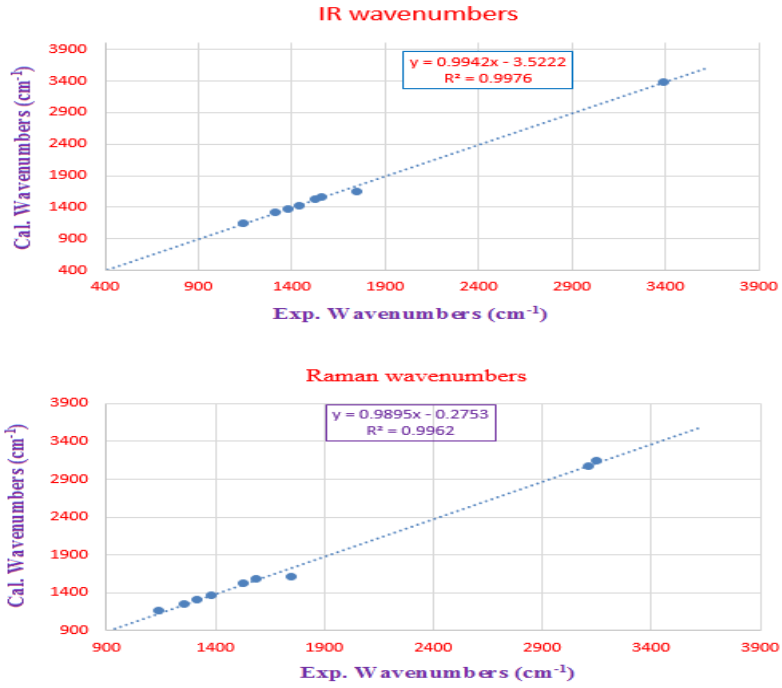

Fig. 4. Correlation graphics between experimental and calculated wavenumbers of -chloro-2-[(furan-2-ylmethyl)amino]-5-sulfamoylbenzoic acid

4.2.1. *NH_2 vibration*

The high frequency region above 3000 cm^{-1} is the characteristic region for the ready identification of C-H, O-H and N-H stretching vibrations. In this region, the bands are not appreciably affected by the nature of the substituents [28]. The investigated molecules have an NH_2 group. Hence, in the NH_2 group, one symmetric and one asymmetric N-H stretching vibration are expected. It is stated that the N-H stretching vibrations occur in the region 3300–3500 cm^{-1} [29]. Specifically, the asymmetric NH_2 stretching vibration appears from 3420 to 3500 cm^{-1} and the symmetric NH_2 stretching is observed in the range 3340–3420 cm^{-1} [29]. Alvareza assigned two strong bands in the IR spectra of liquid sulfamoyl fluoride and sulfamoyl chloride substances at 3418 cm^{-1}, 3312 cm^{-1}, 3386 cm^{-1} and 3282 cm^{-1} [25, 30]. These bands were assigned to the NH_2 antisymmetric and symmetric fundamental stretching of 4-X-sulfamoylbenzoic acid (X = F, Cl, Br, respectively) and were recorded at 3261, 3266, 3240 cm^{-1} and 3361, 3351, 3330 cm^{-1} [31]. In this study, the symmetric NH_2 stretching modes of the studied compounds were recorded in both FT-IR and FT-Raman spectra. The corresponding symmetric mode was observed at 3380 cm^{-1} in the FT-IR. The theoretically computed values by the B3LYP/6-31G(d,p) method were at 3484 and 3386 cm^{-1}. As expected, these two modes are pure stretching modes as is evident from the TED column, and they are almost contributing 100 %. The vibrational NH_2 scissoring deformation appears in the 1638–1575 cm^{-1} region with a strong to very strong IR intensity [32]. The strong bands in FT-IR, and relatively weak bands in FT-Raman, falling in the range 1520–1542 cm^{-1} and described by modes 16 and 17, were assigned to NH_2 scissoring. The NH_2 vibrations such as wagging, rocking, and twisting, are gathered in Table 2. The stretching bands between the sulfur atom and the NH_2 group were also assigned, based on the TED calculations. However, the bands observed 820 and 822 cm^{-1} in FT-IR and FT-Raman.

4.2.2. *C-H Vibration*

The aromatic compounds commonly exhibit multiple weak bands in the region 3000–3100 cm^{-1} [33–35]. In the present study, the hydrogen atoms around the ring give rise to the C-H stretching modes (modes no. 40–44). As expected, all stretching vibrations are very pure modes since their TED contributions are greater than 85 %. The calculations also show very good agreement with the experimental results for the furosemide compound. In the aromatic compound, the C-H in-plane bending frequencies appear in the range of 1000–1300 cm^{-1} and the C-H out-of-plane bending vibrations in the range 750 to 1000 cm^{-1} [34]. In this work, the in-

plane bending vibrations were recorded in the range 1377–1140 cm^{-1} and the out-of-plane bending vibrations in the range 796–1004 cm^{-1}. If we consider the TED calculations, the in-plane bending vibrations are mixed modes and the out-of-plane bending vibrations are assigned as pure modes. The change in the frequency of these deformations from the values in benzene is determined, almost exclusively, by the relative position of the substituents and is almost independent of their nature [36].

4.2.3. *CH_2 group vibrations*

For the assignments of CH_2 group frequencies, basically six fundamentals can be associated to each CH_2 group, namely: CH_2 symmetric stretching; CH_2 asymmetric stretching; CH_2 scissoring, and CH_2 rocking which belongs to in-plane vibrations and two out-of-plane vibrations, viz: CH_2 wagging and CH_2 twisting modes, which are expected to be depolarized [37]. The asymmetrical CH_2 stretching vibrations are generally observed above 3000 cm^{-1}, while the symmetric stretch will appear in the region between 3000 and 2900 cm^{-1} [38, 39]. In this study, the asymmetric and symmetric stretching vibrations are observed at 3107, 2930 and 2880 cm^{-1} respectively, in FT-Raman. For n-alkyl benzenes, the assignments of the C–C stretching mode at about 1464 cm^{-1} and 1290 cm^{-1} are quite problematic, since these bands are frequently masked by the CH_2 scissoring and wagging vibrations, respectively [40, 41]. For furosemide, the CH_2 scissoring mode has been assigned at 1456 cm^{-1} in FT-IR and 1454 cm^{-1} in the FT-Raman spectrum**.** The band at 1375 cm^{-1} in both the IR and Raman is assigned to the CH_2 rocking in-plane vibration [42]. The CH_2 wagging vibrations are observed at 1032, 984 and 906 cm^{-1} in the FT-IR spectra.

4.2.4. *SO_2 vibration*

The asymmetric stretching for the SO_2, NH_2, NO_2, CH_2 and CH_3, etc. has a magnitude higher than the symmetric stretching [43, 32]. The symmetric and asymmetric SO_2 stretching vibrations occur in the regions of 1125–1150 cm^{-1} and 1295–1330 cm^{-1} [29]. The symmetric S=O stretching vibrations at 1096 and 1095 cm^{-1}, by the DFT calculations, are seen as pure modes [44], while these bands were obtained at 1153 and 1146 cm^{-1} in the FT-IR spectrum [45]. Dodoff [46] recorded the symmetric stretching mode at 1150 cm^{-1} as a strong peak, and the antisymmetric modes at 1341 and 1351 cm^{-1} in the infrared spectrum for *N*-3-pyridinylmethanesulfonamide. In this study, the symmetric S=O stretching vibration was at 1064 cm^{-1} in the infrared spectrum. The bands observed at 1310 and 1251 cm^{-1} in the FT-Raman spectrum, and 1316 cm^{-1} in the FT-IR spectrum, were assigned to antisymmetric S=O stretching vibrations. A coincidence between the experimental values with those of the literature [44–46] and the theoretical results are found for the above conclusions. The bending vibrations of O=S=O also given in Table 2.

4.2.5. *C-Cl vibration*

The C-X (X = Cl, F, Br, I) group generally gives strong bands in the frequency range 1130-480 cm^{-1}. The position of the bands is influenced by neighboring atoms or groups. i.e. their frequencies depend on the mass and bond strength of the substitutions. Thus, the smaller the halide atom the greater is the influence of the neighbor. In mono-chlorobenzene derivatives, such as in 4-chloro-3-nitrobenzonitrile [47] and 2-amino-5-chlorobenzonitrile [48], the C-Cl stretching frequency mainly appears in the 800–600 cm^{-1} region [40, 49]. Whereas, in dichlorobenzene derivatives, such as 2-amino-3,5-dichlorobenzonitrile [50], the C-Cl stretching is observed in the range 1100–400 cm^{-1}.

4.2.6. *C-C vibration*

The ring carbon-carbon stretching vibration occurs in the region 1625–1430 cm^{-1}. In general, the bands are of variable intensity and are observed at 1690–1650 cm^{-1}, 1590–1575 cm^{-1}, 1540–1470 cm^{-1}, 1465–1430 cm^{-1} and 1301–1280 cm^{-1}, as given by Varsanyi [51] for the fine bands in this region. In the present work, the wavenumbers of the very strong band observed in the FT-IR spectrum at 1650, 1556, 1423, 1373 and 1316 cm^{-1} have been assigned to the C-C stretching vibrations in furosemide. The same vibrations appear in the FT-Raman spectrum for furosemide at 1607, 1583, 1370, 1310 and 1251 cm^{-1}. The theoretically computed values for furosemide by B3LYP/6-31G(d,p) methods at 1748, 1595, 1583, 1554, 1437, 1377, 1312 and 1271cm^{-1} showed excelled agreement with the experimental data. The in-plane deformation vibration is at higher wave numbers than the out-of-plane vibrations. Shimanouchi et al. [52] gave the wave numbers data for these vibrations for different benzene derivatives from normal coordinate analysis. The theoretically computed values by the DFT method show excellent agreement

with the experimental data. Small changes observed in the wavenumbers for these modes are due to the change in force constant/reduced mass ration resulting mainly from the extent of mixing between the ring and the substitution group [53].

4.3. *UV-VIS spectral analysis*

The time dependent density functional method (TD-DFT) is able to detect accurate absorption wavenumbers at a relatively small computing time which corresponding vertical electronic transitions computed on the ground state geometry, especially in the study of the solvent effect [54–56]. Experimentally, the electronic transitions bands were at 230 and 305 nm. Theoretically, the three intense electronic transitions were predicted at 269.58 nm (f = 0.0000), 315.99 nm (f = 0.0117), and 324.13 nm (f = 0.0893), which agree with the experimental data. The molecular orbitals involved in these electronic transitions are shown in Figure 5. Both electronic transitions are $\pi \rightarrow \pi^*$ excitations.

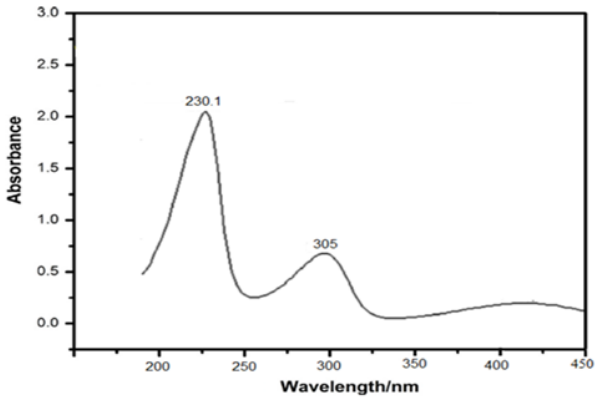

Fig. 5. Experimental UV-Vis spectra of 4-chloro-2-[(furan-2-ylmethyl)amino]-5-sulfamoylbenzoic acid using TD-DFT/B3LYP/6-31G(d,p) method.

4.4. *Frontier molecular orbital analysis*

Molecular orbitals (HOMO and LUMO) and their properties, such as energy, are very useful for physicists and chemists and are very important parameters for quantum chemistry. This is also used by the frontier electron density for predicting the most reactive position in π-electron systems, and also explains several types of reaction in conjugated systems [57]. The conjugated molecules are characterized by a small highest occupied molecular orbital-lowest unoccupied molecular orbital (HOMO-LUMO) separation, which is the result of a significant degree of intramolecular charge transfer from the end-capping electron-donor groups to the efficient electron-acceptor groups through the π conjugated path [58]. Both the highest occupied molecular orbital-lowest unoccupied molecular orbital are the main orbitals that takes part in chemical stability [59].

The HOMO represents the ability to donate an electron, and LUMO as an electron acceptor represents the ability to obtain an electron. The HOMO and LUMO energy calculated by the B3LYP/6-31G(d,p) method is shown below. This electronic absorption corresponds to the transition from the ground to the first excited state and is mainly described by one electron excitation from the highest occupied molecular orbital to the lowest unoccupied molecular orbital. While the energy of the HOMO is directly related to the ionization potential, LUMO energy is directly related to the electron affinity. The energy difference between the HOMO and LUMO orbitals is called the energy gap and is an important stability for structures [60]. Recently, the energy gap between HOMO and LUMO has been used to prove the bioactivity from intramolecular charge transfer [61, 62]. The plots of the highest HOMOs and LUMOs are shown in Figure 6.

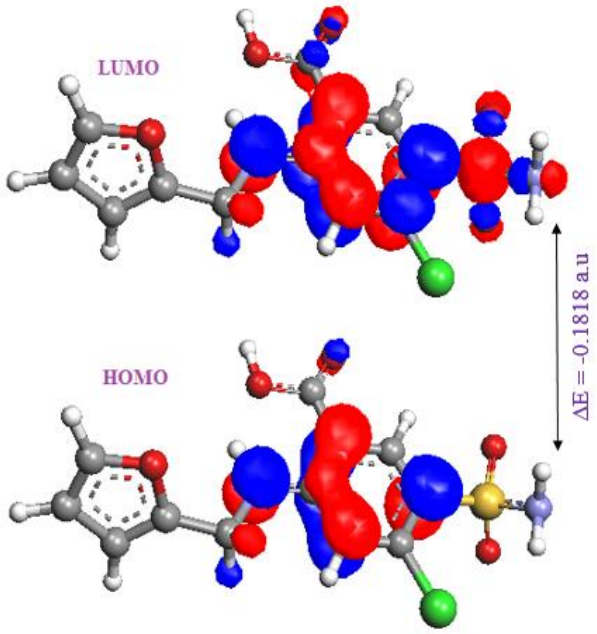

Fig. 6. Frontier molecular orbital of 4-Chloro-2-[(furan-2-ylmethyl)amino]-5-sulfamoylbenzoic acid molecule

The HOMO is located over the chlorosulfamoyl benzoic acid ring, and the HOMO→LUMO transition implies an electron density transfer to the amino group from the chlorosulfamoyl benzoic acid ring and lower in the HOMO and LUMO energy gap explains the eventual

charge transfer interactions taking place within the molecule

HOMO energy (B3LYP) = –0.24699 a.u

LUMO energy (B3LYP) = –0.06519 a.u

HOMO–LUMO energy gap (B3LYP) = –0.1818 a.u

4.5. *Global reactivity descriptors*

Based on the density functional descriptors, global chemical reactivity descriptors of the furosemide molecule such as ionization potential (I), electron affinity (A), chemical potential (μ), electronegativity (χ), global hardness (η), global softness (σ) and global electrophilicity (ω) values can be described as follows [63, 64]. In simple molecule orbital theory approaches, the HOMO energy (E_{HOMO}) is related to the ionization potential by Koopman's theorem and the LUMO energy (E_{LUMO}) has been used to estimate the electron affinity.

$$I = -E_{HOMO}$$

$$A = -E_{LUMO}$$

The average value of the HOMO and LUMO energy is related to the electronegativity defined by Mulliken [67].

$$\chi = (I+A)/2$$

In addition, the HOMO and LUMO energy is related to the hardness (η) and softness (σ) [60]

$$\eta = (I-A)/2$$

$$\sigma = 1/\eta$$

Global electrophilicity (ω) is defined as: [65]

$$\omega = -\mu^2/2\eta$$

where μ is the chemical potential which takes the average value of the ionization potential (I) and electron affinity (A) [66]

$$\mu = -(I+A)/2$$

The electronic chemical potential is the parameter which describes the tendency of electrons to escape from an equilibrium system. Thus, the frontier molecular orbital analysis also provides details on the chemical stability, chemical hardness and electronegativity of the molecule, the results of which from the B3LYP/6-31G(d,p) basis set are presented in Table 3.

T a b l e 3

Comparison of HOMO, LUMO energy gaps and related molecular properties of 4-Chloro-2-[(furan-2-ylmethyl)amino]-5-sulfamoylbenzoic acid at B3LYP/6-3G(d,p) level of theory

Molecular Properties	Energy (a.u)	Energy gap (eV)	Ionization potential (I)	Electron affinity (A)	Global hardness (η)	Electro negativity (χ)	Global softness (σ)	Chemical potential (μ)	Global electriphilicity (ω)
B3LYP/6-311G(d,p)									
HOMO	–0.24699	–0.1818	0.1818	0.0651	0.0583	0.1234	17.1526	–0.0583	0.4848
LUMO	–0.06519								
HOMO	–0.24699	–0.21972	0.2197	0.0272	0.0962	0.1234	10.3950	–0.0962	0.4972
LUMO+1	–0.02727								
HOMO	–0.24699	–0.23621	0.2362	0.0107	0.1127	0.1234	8.8731	–0.1127	0.5000
LUMO+2	–0.01073								

4.6. *Mulliken analysis*

Charge distributions of the molecules have been calculated by performing a Mulliken analysis [67].The theoretically calculation of atomic charges plays an important role in the application of quantum mechanical calculations to molecular systems. The calculated results reveal that the negative charge is delocalized between the carbon and nitrogen atoms. For the hydrogen atoms, the differences in the calculated charges are relatively smaller. It is worth mentioning that the largest values of charge are noticed for H24 and H27 which are involved in hydrogen bonding (0.3356e and 0.3051e, respectively). Large values of charge on N3 (negative) and S10 (positive) are due to the intramolecular charge transfer which occurs within the molecule. Figure 7 shows that the natural atomic charges are more sensitive to the changes in the molecular structure than Mulliken's net charges.

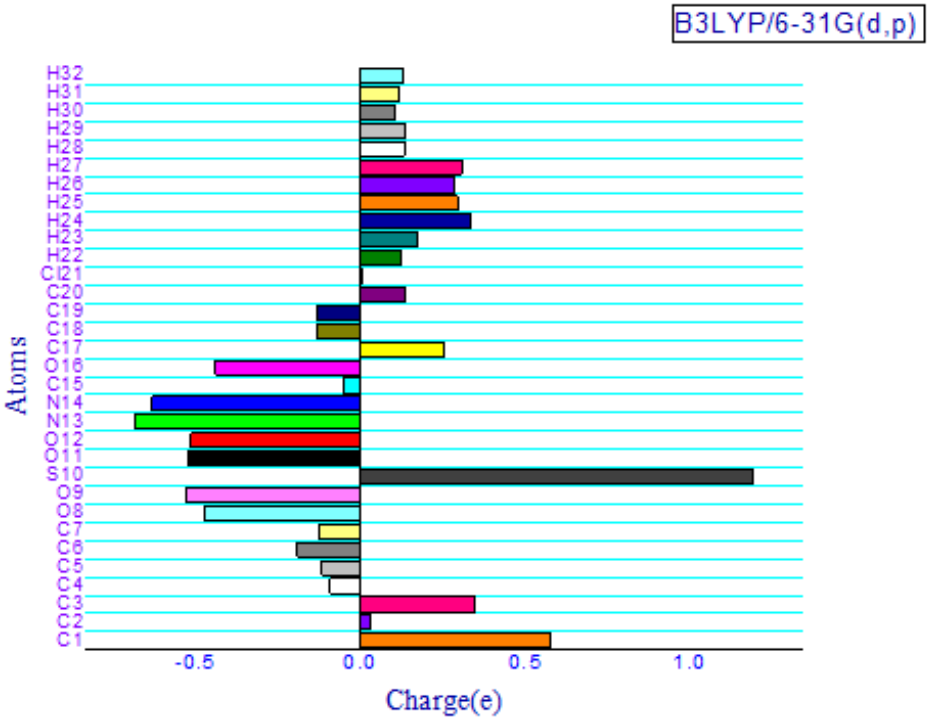

Fig. 7. The historam of calculated Mulliken charge for 4-chloro-2-[(furan-2-ylmethyl)amino]-5-sulfamoylbenzoic acid molecule

4.7. *Molecular electrostatic potential*

Molecular electrostatics is used extensively for interpreting potentials and predicting the reactive behavior of a wide variety of chemical systems in both electrophilic and nucleophilic reactions, the study of biological recognition processes, and hydrogen bonding interactions [68]. To predict reactive sites for electrophilic and nucleophilic attack for the investigated compound, the Molecular Electrostatic Potential (MEP) was calculated at B3LYP/6-31G(d,p). The different values of the electrostatic potential at the surface are represented by different colors; red represents the region of most electro-negative electrostatic potential, blue represents the region of the most positive electrostatic potential, and green represents the region of zero potential. The potential decreases in the order red < orange < yellow < green < blue. The MEP surface provides the necessary information about the reactive sites. The total electron density on to which the MEP has been mapped is shown in Fig.8 This figure provides a visual representation of the chemically active sites and the comparative reactivity of the atoms [69]. The electrophilic reactivity is related to the negative region and the nucleophilic reactivity is related to the positive one, as can be seen from the MEP of the candidate molecule. The major positive potential region around the hydrogen atom of the hydroxyl group, characterized by a blue color, indicates the site for nucleophilic attack while rest of the region is almost neutral, characterized by the green color.

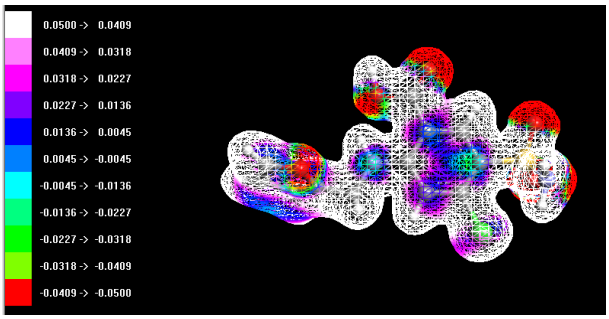

Fig. 8. 3D plots of the molecular electrostatic potential for 4-Chloro-2-[(furan-2-ylmethyl)amino]-5-sulfamoylbenzoic acid molecule

4.8. *Thermodynamic analysis*

In order to understand the thermodynamic behavior of the furosemide compound, the thermodynamic parameters (such as zero point vibrational energy, thermal energy, specific heat capacity, rotational constants, entropy and dipole moment) of 4M4M2PO were calculated by DFT/B3LYP method using 6-31G basis set at 298.15 K and 1 atm pressure, and are presented in Table 4. These functions describe the thermodynamic stability of the system at given conditions of pressure and temperature [70].

T a b l e 4

Calculated thermodynamic parameters of 4-chloro-2-[(furan-2-ylmethyl)amino]-5-sulfamoylbenzoic acidat 298.15 K

Parameters	B3LYP/6-3G(d,p)
SCF energy (a.u)	-1807.822
Total energy + ZPE (AU)	0.229
Gibbs Free energy (AU)	0.178
Rotational constants (GHz)	0.889
	2.981
	35.142
Entropy (cal mol^{-1} K^{-1})	
Total	156.034
Translational	0.889
Rotational	0.889
Vibrational	154.257
Dipole moments, μ (Debyes)	$\mu_x = -9.151$
	$\mu_y = -2.424$
	$\mu_z = 3.259$
	$\mu_{Total} = 10.012$

The dipole moment of a molecule is an important property and it helps to study the intermolecular interactions involving the non-bonded type dipole-dipole interactions, because the higher the dipole moment, the stronger the intermolecular interactions [71]. Furthermore, the dipole moment can be used to describe the charge movement across the molecule. The direction of the dipole moment vector in a molecule depends on the centers of negative and positive charges. The dipole moment of furosemide obtained in 6-31G basis set is 10.012 D.

5. CONCLUSIONS

In the present study, the molecular structure and vibrational frequencies have been studied using DFT (B3LYP) calculations with the 6-31G(d,p) basis set. The final optimized structure is in good agreement with the experimental structure. The experimental derivations between the models can be attributed to the differences between the calculation and the experimental measurements, i.e., gas phase and solid phase. The FT-IR and FT-Raman spectra of the studied compound were calculated and assigned based on the total energy distribution. The calculations show that using the TD-DFT/6-31G(d,p) approach, the experimental absorption spectrum has been well reproduced. It has been concluded that the lowest singlet excited state of the furosemide molecule is mainly derived from the HOMO→LUMO ($\pi \rightarrow \pi^*$) electronic transitions. A molecular electrostatic potential map and global reactivity parameters were used to describe the chemical reactivity of the studied molecule.

REFERENCES

[1] F. O. Simsek, M. S Kaynak, N. Sanil & S. Sahin, Determination of amlodipine and furosemide with newly developed and validated RP-HPLC method in commercially available tablet dosage forms, *Hacettepe University Journal of the Faculty of Pharmacy*, **32(2),** 145–158 (2012).

[2] C. T. Supuran, A. Scozzafava, Carbonic anhydrase inhibitors, *Curr. Med. Chem., Immunol., Endocrine Metabolic Agents*, **1**, 61–97 (2001). DOI: 10.2174/1568013013359131

[3] C. T. Supuran, A. Scozzafava, A. Casini, Carbonic anhydrase inhibitors, *Med. Res. Rev.,* **23**, 146–189 (2003). DOI: 10.1002/med.10025

[4] C. T. Supuran, A. Scozzafava, Applications of carbonic anhydrase inhibitors and activators in therapy, *Expert Opin. Ther. Patents*, **12**, 217–242 (2002). DOI.org/10.1517/13543776.12.2.217

[5] J. Niessen, U. Schoder, M. Rosenbaum, F.Scholz, Fluorinated polyanilines as superior materials for electrocatalytic anodes in bacterial fuel cells, *Electrochemistry Communications*, **3,** 571–575 (2004). DOI.org/10.1016/j.elecom.2004.04.006

[6] N. Sundaraganesan, J. Karpagam, S. Sebastian, J. P. Cornard, The spectroscopic (FTIR, FT-IR gas phase and FT-Raman), first order hyperpolarizabilities, NMR analysis of 2,4-dichloroaniline by ab initio HF and density functional methods, *Spectrochimica Acta Part A: Molecular and Biomolecular Spectroscopy*, **73**, 1119–1122 (2009). DOI.org/10.1016/j.saa.2009.01.007

[7] M. Karabacak, D. Karagoz, M. Kurt, Experimental (FT-IR and FT-Raman spectra) and theoretical (ab initio HF, DFT) study of 2-chloro-5-methylaniline, *Journal of Molecular Structure*, **892,** 25–31 (2008). DOI.org/10.1016/j.molstruc.2008.04.054

[8] A. Altun, K. Golcuk, M. Kumru, Structure and vibrational spectra of p-methylaniline: Hartree-Fock, MP2 and density functional theory studies, *Journal of Molecular Structure: THEOCHEM*, **637**, 155–169 (2003). DOI.org/10.1016/S0166-1280(03)00531-1

[9] M. Govindarajan, M. Karabacak, S. Periandy, D. Tanuj, Spectroscopic (FT-IR, FT-Raman, UV and NMR) investigation and NLO, HOMO–LUMO, NBO analysis of organic 2,4,5-trichloroaniline, *Spectrochimica Acta Part A: Molecular and Biomolecular Spectroscopy*, **97**, 231–245 (2012). DOI.org/10.1016/j.saa.2012.06.014

[10] M. Karabacak, D. Karagoz, M. Kurt, FT-IR, FT-Raman vibrational spectra and molecular structure investigation of 2-chloro-4-methylaniline: A combined experimental and theoretical study, *Spectrochimica Acta Part A: Molecular and Biomolecular Spectroscopy*, **72**, 1076–1083 (2009). DOI.org/10.1016/j.saa.2008.12.047

[11] P. Wojciechowski, K. Helios, D. Michalska, *Vib. Spectr*., **57**, 126–134 (2011).

[12] H. Wang, B. Liu, J. Wan, J. Xu, X. Zheng, Excited-state structural dynamics and vibronic coupling of 1,3-dithiole-2-thione—resonance Raman spectroscopy and density functional theory calculation study, *J. Raman Spectrosc*, **40**, 992–997 (2009). DOI: 10.1002/jrs.2216

[13] H. Wang, J. Xu, J. Wan, Y. Zheno, X. Zheng, Excited state structural dynamics of tetra(4-aminophenyl)porphine in the condensed phase: resonance Raman spectroscopy and density functional theory calculation study, *J. Phys Chem. B*, **114**, 3623–3632 (2010). DOI: 10.1021/jp1000978

[14] Gaussian Inc., Gaussian 09 Program, Gaussian Inc., Wallingford, 2009.

[15] H. B. Schlegel, Optimization of equilibrium geometries and transition structures, *J. Comput. Chem*., **3**, 214–218 (1982). DOI: 10.1002/jcc.540030212

[16] J. Baker, A. A. Jarzecki, P. Pulay, Direct scaling of primitive valence force constants: An alternative approach to scaled quantum mechanical force fields, *J. Phys. Chem.,* **102 A,** 1412–1424 (1998). DOI: 10.1021/jp980038m

[17] P. Pulay, J. Baker, K. Wolinski, Reply to the comments on Efficient calculation of canonical MP2 energies' by A. Kohn and C. Hattig, *Chem. Phys. Lett.*, **358**, 354–356 (2002). DOI.org/10.1016/S0009-2614(02)00610-3

[18] F. Weinhold, Gauss view, *J. Am. Chem. Phys. Soc*., **102,** 7211 (1980).

[19] J. V. Prasad, S. S. Rai, S. N. Thakuk, Overtone spectroscopy of benzene derivatives using thermal lensing, *Chem. Phys. Lett.* **164 (6),** 629–634 (1989). DOI.org/10.1016/0009-2614(89)85272-8

[20] K. M. Gough, B. R. Henry, Carbon-hydrogen stretching overtone spectra of nitrobenzene and its deuterated derivatives. Assignment of the ortho carbon-hydrogen bond, *J. Phys. Chem.*,**87**, 3804–3805 (1983). DOI: 10.1021/j100243a003

[21] M. K. Ahmed, B. R. Henry, Gas-phase overtone spectral investigation of structurally and conformationally nonequivalent carbon-hydrogen bonds in trimethylbenzenes, *J. Phys. Chem.* **90**, 1737–1739 (1986). DOI: 10.1021/j100400a002

[22] M. S. Dewar, P. J. Grisdale, *J. Am. Chem. Soc*. **84**, 3539 (1962).

[23] B. G. Johnson, P. M. Gill, J. A. Pople, The performance of a family of density functional methods, *J. Chem. Phys.*, **98**, 5612 (1993). DOI.org/10.1063/1.464906

[24] B. T. Gowda et al., *ActaCryst*. **E63**, 2967 (2007).

[25] B. M. S. Alvareza, M. I. M. Valdeza, E. H. Cultin, C. O. D. Vedova, Spectroscopic and theoretical studies of sulfamoil fluoride, FSO_2NH_2 and N-(fluorosulfonyl) imidosulfuryl fluoride, $FSO_2NS(O)F_2$, *J.Mol.Struct.,* **657**, 291–300 (2003). DOI.org/10.1016/S0022-2860(03)00407-1

[26] M. F. Erben, C. O. D. Vedova, R. Boese, H. Willner, C. Leibold, H. Oberhammer, Trifluoromethyl chlorosulfonate, CF_3OSO_2Cl: Gas phase and crystal structure, conformation and vibrational analysis studied by experimental and theoretical methods, *Inorganic chemistry*, **42**, 7297–7303 (2003). DOI: 10.1021/ic034531a

[27] M. E. Tuttolomondo, P. E. Arganaraz, E. L. Varetti, S. A. Hayes, D. A. Wann, H. E. Robertson, D. W.N. Rankin, A. B. Altabef, Gas-phase structure and vibrational properties of trifluoromethyl trifluoromethanesulfonate, $CF_3SO_2OCF_3$, *Eur. J. Inorg. Chem*., **10,** 1381–1389 (2007). DOI: 10.1002/ejic.200600940

[28] M. Silverstein, G. C. Basseler, C. Morill, Spectrometric identification of organic compounds, *Wiley*, Newyork, 1981.

[29] L. J. Bellamy, The Infrared Spectra of Complex Molecules, vol.2, *Chapman and Hall*, London, 1980.

[30] R. M. S. Alvareza, E. H. Cutin, C. O. D. Vedova, Vibrational studies of sulfamoil chloride ($ClSO_2NH_2$), *J. Mol. Struct*. **440**, 213–219 (1998). DOI.org/10.1016/S0022-2860(97)00260-3

[31] B. T. Gowda, K. Jyothi, J. D. D. Souza, *Journal for Nature Research*, 57a (2002) 967–973.

[32] D. Lin-Vien, N. B. Colthup, W. G. Fateley, J. G. Grasselli, The Handbook of Infrared and Raman Characteristic Frequencies of Organic Molecules, *Academic Press*, Boston, MA, 1974.

[33] M. Silverstein, G. C. Basseler, C. Morill, Spectrometric identification of organic compounds, *Wiley*, New York, 1981.

[34] G. Varsanyi, Assignments of vibrational spectra of 700 benzene derivatives, *Wiley*, New York, 1974, pp. 280.

[35] A. Altun, K. Golcuk, M. Kumru, Theoretical and experimental studies of the vibrational spectra of m-methylaniline, *J. Mol. Struct. (Theochem.)*, **625**, 17–24 (2003). DOI.org/10.1016/S0166-1280(02)00698-X

[36] N. Sundaraganesan, H. Saleem, S. Mohan, Vibrational spectra, assignments and normal coordinate analysis of 3-aminobenzyl alcohol, *Spectrochim. Acta A*, **59**, 2511–2517 (2003). DOI.org/10.1016/S1386-1425(03)00037-4

[37] N. B. Colthup, L. H. Daly, S. E. Wiberley, *Introduction to Infrared and Raman spectroscopy*, Academic Press, New York, 1990.

[38] S. Muthu, E. I. Paulraj, *Solid State Sci*., **14**, 476–487 (2012).

[39] D. Sajan, J. Binoy, B. Pradeep, K. V. Krishna, V. B. Kartha, I. H. Joe, V. S. Jayakumar, *Spectrochim. Acta A* **60**, 173–180 (2004).

[40] S. Muthu, N. R. Sheela, S. Sampathkrishnan, *Mol. Simul*., **37**, 1276–1288 (2011).

[41] K. B. Wiberg, A. Sharke, *Spectrochim. Acta A*, **29**, 583–594 (1973).

[42] V. Krishnakumar, N. Surumbarkuzhali, S. Muthunatesan, *Spectrochim. Acta A*, **71,** 1810–1813 (2009).

[43] M. Karabacak, M. Cinar, Z. Unal, M. Kurt, FT-IR, UV spectroscopic and DFT quantum chemical study on the molecular conformation, vibrational and electronic transitions of 2-aminoterephthalic acid, *J.Mol.Struct.*, **982** 22–27 (2010). DOI.org/10.1016/j.molstruc.2010.07.033

[44] M. Karabacak, M. Cinar, M. Kurt, DFT based computational study on the molecular conformation, NMR chemical shifts and vibrational transitions for N-(2-methylphenyl) methanesulfonamide and N-(3-

methylphenyl) methanesulfonamide, *J. Mol. Struct*, **968**, 108–114 (2010). DOI.org/10.1016/j.molstruc.2010.01.033

[45] K. L. Jayalaksmi, B. T. Gowda, Synthetic, infrared and NMR (^{1}H and ^{13}C) spectral studies of n-(substituted phenyl)-methanesulphonamides, *Journal for Nature Research*, **59a,** 491–500 (2004). DOI: 0932–0784 / 04 / 0700–049

[46] N. I. Dodoff, *Vib. Spectrosc*. **4(3)**, 5–9 (2000).

[47] Y. Sert, C. Cirak, F. Ucun, Vibrational analysis of 4-chloro-3-nitrobenzonitrile by quantum chemical calculations, *Spectrochim. Acta A*, **107,** 248–255 (2013). DOI.org/10.1016/j.saa.2013.01.046

[48] B. Lakshmaiah, G. R. Rao, Vibrational analysis of substituted anisoles. I–Vibrational spectra and normal coordinate analysis of some fluoro and chloro compounds, *J. RamanSpectrosc.*, **20**, 439-448 (1989). DOI: 10.1002/jrs.1250200709

[49] J. A. Fanitan, I. Iweibo, R. A. Oderinde. *J. Raman Spectrosc*. **11**, 6 (1998).

[50] V. K. Rastogi, M. Alcolea Palafox, R. Tomar, 2-Amino-3,5-dichlorobenzonitrile: DFT calculations in the monomer and dimer forms, FT-IR and FT-Raman spectra, molecular geometry, atomic charges and thermodynamical parameters, *Spectrochim Acta A*, **110**, 458-470 (2013). DOI.org/10.1016/j.saa.2013.03.026

[51] G. Varsanyi, *Assignments of Vibrational Spectra of Benzene Derivatives*, Academic Press, New York, 1969.

[52] T. Shimanouchi, Y. Kalkiuti, I. Gamo, Stability and burning velocities of laminar carbon monoxide-air flames at pressures up to 93 atmospheres, *J. Chem. Phys.* **25**, 1241–1245 (1956). DOI.org/10.1063/1.1743186

[53] V. Balachadran, V. Karpagam, A. Lakshmi, Conformational stability, theoretical and experimental vibrational spectral analysis of 2,4,6-trihydroxybenzaldehyde, *J. Mol. Struct.* **1021**, 13–21 (2012). DOI.org/10.1016/j.molstruc.2012.04.070

[54] D. Jacquemin, J. Preat, E. A. Perpete, A TD-DFT study of the absorption spectra of fast dye salts, *Chem. Phys. Lett.* **410**, 254–259 (2005). DOI.org/10.1016/j.cplett.2005.05.081

[55] D. Jacquemin, J. Preat, M. Charlot, V. Wathelet, J. M. Andre, E. A. Perpete, Theoretical investigation of substituted anthraquinone dyes, *J. Chem. Phys.* **121** 1736–1746 (2004). DOI: 10.1063/1.1764497

[56] M. Cossi, V. Barone, Time-dependent density functional theory for molecules in liquid solutions, *J. Chem. Phys.*, **115,** 4708 (2001). DOI.org/10.1063/1.1394921

[57] K. Fukui, T. Yonezewa, H. Shingu, A molecular orbital theory of reactivity in aromatic hydrocarbons, *J. Chem. Phys*, **20**, 722 (1952). DOI.org/10.1063/1.1700523

[58] C. H. Choi, M. Kertesz, Conformational Information from Vibrational Spectra of Styrene, trans-Stilbene, and cis-Stilbene, *J. Phys. Chem.* **101 (20),** 3823–3831 (1997). DOI: 10.1021/jp970620v

[59] S. Gunasekeran, R. A. Balaji, S. Kumeresan, G. Anand, S. Srinivasan, Experimental and theoretical investigations of spectroscopic properties of N-acetyl-5-methoxytryptamine, *Can. J. Anal. Sci. Spectrosc*, **53**, 149–160 (2008).

[60] D. F. Lewis, C. Loannides, D. V. Pake, Interaction of a series of nitriles with the alcohol-inducible isoform of P450: Computer analysis of structure—activity relationships, *Xenobiotica*, **24**, 401–408 (1994). DOI.org/10.3109/00498259409043243

[61] L. Padmaja, C. Ravikumar, D. Sajan, I. H. Joe, V. S. Jayakumar, G. R. Pettit, O. F. Nielson, Density functional study on the structural conformations and intramolecular charge transfer from the vibrational spectra of the anticancer drug combretastatin–A2, *J. Raman Spectrosc*, **40**, 419–428 (2009). DOI: 10.1002/jrs.2145

[62] C. Ravikumar, I. H. Joe, V. S. Jayakumar, Charge transfer interactions and nonlinear optical properties of push–pull chromophore benzaldehyde phenylhydrazone: a vibrational approach, *Chem. Phys. Lett.* **460**, 552–558 (2008). DOI.org/10.1016/j.cplett.2008.06.047

[63] P. Politzer & J. S. Murray, The fundamental nature and role of the electrostatic potential in atoms and molecules, *Theor. Chem. Acc.*, **108**, 134–142 (2002). DOI.org/10.1007/s00214-002-0363-9

[64] R. G. Pearson, *Chemical Hardness*, John Wiley-VCH, Weinheim, New York , 1997.

[65] R. G. Parr, V. Laszlo, Szentpály & S. Liu, Electrophilicity Index, *J. Am. Chem. Soc*, **121**, 1922–1924 (1999). DOI: 10.1021/ja983494x

[66] J. Padmanabhan, R. Parthasarathi, V. Subramanian & P.K. Chattaraj, Electrophilicity-based charge transfer descriptor, *J. Phys. Chem*, A, **111**, 1358–1361 (2007). DOI: 10.1021/jp0649549

[67] R. S. Mulliken, Electronic population analysis on LCAO–MO molecular wave functions. I, *J. Chem. Phys*, **23**, 1833–1840 (1955). DOI.org/10.1063/1.1740588

[68] P. Polizer, J. S. Murry, Theoretical biochemistry and molecular biophysics: a comprehensive survey, in: D. I. Beveridge, R. Lavery (Eds.), *Electrostatic Potential Analysis of Dibenzo –p-dioxins and Structurally Similar System in Relation to Their Biological Activities*, Protein, Vol.2, Academic Press, Schenectady, NY, 1991, Chapter 13

[69] V. P. Gupta, A. Sharma, V. Virdi, V. J. Ram, Structural and spectroscopic studies on some chloropyrimidine derivatives by experimental and quantum chemical methods, *Spectrochim Acta Part A*, **64**, 57–67 (2006). DOI.org/10.1016/j.saa.2005.06.045

[70] Z. Ran, D. Baotong, S. Gang, S. Yuxi, Experimental and theoretical studies on o-, m- and p-chlorobenzylideneaminoantipyrines, *Spectrochim Acta Part A*, **75,** 1115–1124 (2010). DOI.org/10.1016/j.saa.2009.12.067

[71] O. Prasad, L. Sinha, N. Kumar, Theoretical Raman and IR spectra of tegafur and comparison of molecular electrostatic potential surfaces, polarizability and hyerpolarizability of tegafur with 5-fluoro-uracil by density functional theory, *J. At. Mol. Sci*, **1**, 201–214 (2010). DOI: 10.4208/jams.032510.042010a